Research Article Vol. 29, No. 6 / 15 March 2021 / Optics Express 8368
Optics EXPRESS

Photon thermalization and a condensation phase transition in an electrically pumped semiconductor microresonator

S. Barland,[1,*] P. Azam,[1] G. L. Lippi,[1] R. A. Nyman,[2] and R. Kaiser[1]

[1] Université Côte d'Azur, CNRS, INPHYNI, 1361 route des Lucioles, 06560 Valbonne, France
[2] Physics Department, Blackett Laboratory, Imperial College London, Prince Consort Road, SW7 2AZ, UK
[*] stephane.barland@univ-cotedazur.fr

Abstract: We report on an experimental study of photon thermalization and condensation in a semiconductor microresonator in the weak-coupling regime. We measure the dispersion relation of light and the photon mass in a single-wavelength, broad-area resonator. The observed luminescence spectrum is compatible with a room-temperature, thermal-equilibrium distribution. A phase transition, identified by a saturation of the population at high energies and a superlinear increase of the occupation at low energy, takes place when the phase-space density is of order unity. We explain our observations by Bose-Einstein condensation of photons in equilibrium with a particle reservoir and discuss the relation with laser emission.

Bose-Einstein condensation (BEC) has been an important topic in both fundamental research and applied physics, with many studies involving superfluidity, superconductivity and ultracold particles. While particle-particle interactions are typically sufficiently strong for thermalization to occur during experimental time scales, direct photon-photon interactions are often too small to allow for thermalization among photons to be observed. To make light reach equilibrium requires the introduction of both a medium which interacts strongly with the light [1] and a gap in the optical density of states to provide an energy minimum in the optical range. Near-planar optical microresonators with mirror spacing of the order of the wavelength can provide the necessary density of states, with a characteristic paraxial parabolic form [2–4] for the dispersion relation.

In semiconductor microresonators, where light and matter coherently interact faster than dissipative processes the condensation of quasi-particles known as polaritons is well established [5–7]. In the highest quality samples, the polariton thermalization rate, compared to the exciton's lifetime, is high enough to show near-equilibrium BEC [8]. In the absence of excitons, light and matter interact mostly incoherently (but potentially very fast) through absorption and emission processes. In semiconductors these processes involve charge carriers and are expected to lead to thermalization if light is given sufficient time to interact with the medium [1]: a photon at high energy absorbed by the medium may be re-emitted at lower energy. Photon BEC has been shown to occur in several experimental devices including fluorescent dyes coupled to optical microresonators [9–11] and plasmonic lattices [12], with excellent agreement with a microscopic theory based on dissipative cavity quantum-electrodynamics [13]. Light has also been shown to thermalize [14] and condense [15] by incoherent interaction with erbium/ytterbium colour centres in optical fibre resonators. In random media [16,17], condensation phenomena have been described in relation to lasing.

Here we observe thermalization and a phase transition displaying hallmarks of photon BEC in an electrically pumped, broad-area (*i.e.*, strongly spatially multimode) semiconductor microresonator in the regime of weak coherent coupling but substantial incoherent coupling. This type of device

#409344 https://doi.org/10.1364/OE.409344
Journal © 2021 Received 29 Sep 2020; revised 12 Feb 2021; accepted 13 Feb 2021; published 3 Mar 2021

Optics EXPRESS

is very widely used, suggesting that photon BEC could be more commonplace than widely believed.

Vertical-Cavity Surface-Emitting Lasers (VCSELs) are a mature semiconductor technology, where coherent optical conversion is efficiently obtained from a heterostructure. They are routinely used in applications including telecommunications, sensing, illumination and heating [18,19]. These devices are typically described as light emitters where the threshold for coherent emission is reached when optical gain compensates losses. Broad-area multimode VCSELs have been analyzed in great depth in the mean-field and semiclassical settings because of their large aspect ratio, which is essential for the analysis of transverse spatial phenomena including optical morphogenesis, localized states and vortices [20–28]. However, no detailed analysis of the spectral properties of these devices in relation to BEC has been yet reported. Three key properties of VCSELs make photon thermalisation and BEC almost inevitable: (i) re-absorption of light in these structures by the gain medium is strong, (ii) the semiconductor medium follows a thermal relation between gain and emission, the van Roosbroeck-Shockley relation [29], and (iii) by construction, broad-area VCSELs are longitudinally single-mode but transversely many mode, so show a low-energy cutoff in the density of states for light.

Here we measure the dispersion relation of light in a broad-area VCSEL and the corresponding effective photon mass in absence of excitons. The luminescence spectrum is compatible with a room-temperature thermal-equilibrium distribution suggesting thermalization of light via interaction with a thermal reservoir. This is confirmed by the phase transition observed at high photon density, identified both by a superlinear increase of the occupation of low energy modes and a saturation in the population of higher-energy levels as the total population is increased. At the transition, the phase-space density is of order unity, as expected for BEC in a flat two-dimensional potential for a finite-sized system.

The experimental device (Fig. 1) consists of a thin layer of quantum-well active material, where the light-matter interaction takes place, enclosed in a microresonator formed by high-reflectivity dielectric mirrors. It is an electrically pumped, 150 μm diameter VCSEL. The material consists of three InGaAs quantum wells embedded in GaAs barriers, themselves surrounded by AlGaAs cladding which serves as spacing to obtain a single-wavelength thickness of the inner resonator. The back and front mirrors are composed of respectively 30 and 24 pairs of $Al_{0.9}Ga_{0.1}As$–GaAs [22,30] with a cavity resonance close to 975 nm. Photons are emitted thanks to electron–hole recombinations in the quantum wells prepared to have a photoluminescence maximum between 980 and 1000 nm under operating conditions, thereby matching the detuning requirements outlined for photon BEC in [13]. Since the device is monolithic, we do not have access to a the luminescence spectrum in absence of resonator effect. The flat mirrors are expected to lead to uniform distributions of electric field and density of states, but current diffusion and insulating barriers lead to a slightly higher rate of photon emission close to the edges due to current crowding [31] (right panel of Fig. 1). The temperature of the device's substrate is actively stabilized at 293 K. Excitons are not formed significantly in GaAs at room temperature and the experiment is performed in the weak-coupling regime.

We analyze the optical spectrum as a function of emission angle using a goniometric setup. The semiconductor micro-resonator is placed at the center of a 7-cm diameter programmable rotation stage. No collimating or focusing optics are used and light is collected by a 200 μm-core (multimode) optical fiber placed about 7 cm from the cavity, ensuring far-field detection (Fraunhofer distance $\approx$ 4 cm). The angular spectral analysis is obtained by rotating the sample around the stage's axis while keeping the optical fiber position and alignment stationary and fixed with respect to the center of the micro-resonator.

The measurement angle is varied over a range of 107.8° in steps of 0.2°, matching the resolution limit set by the fiber diameter and propagation distance. For each angle we measure an optical spectrum in the interval 940.0 nm $\leq \lambda \leq$ 980.7 nm (i.e. 1.264–1.319 eV). The color-coded

Optics EXPRESS

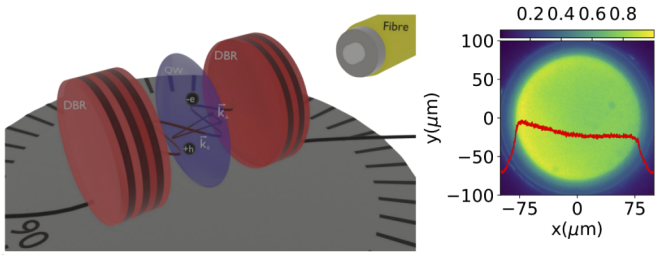

Fig. 1. Schematics of the experimental platform: light is confined in a 150 μm diameter and 1-λ-long microresonator closed by flat high-reflectivity dielectric mirrors where an electrically pumped thin layer of quantum wells provides nonlinearity (device details available in [30]). After 7 cm free space propagation, light is collected by a multimode optical fiber. Right: color-coded image of light emitted from the front-facing mirror, the red line is a cut along the horizontal diameter.

spectra (resolution 0.1 nm, Fig. 2, left) are shown as a function of the emission angle. The short and planar resonator with large aspect ratio allows us to observe the parabolic shape expected in a Fabry-Perot cavity for the transverse component of the light's dispersion relation [2,3] over a remarkably large emission angle ($\approx 86°$). We attribute the asymmetry between the two sides at large emission angles to inhomogeneous current distribution (Fig. 1, right).

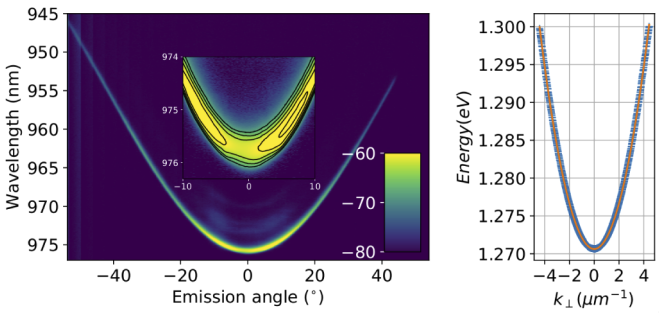

Fig. 2. Dispersion relation measurement. Left: color-coded emission spectra in dBm with angular resolution (pumping current 150 mA, near threshold). Inset: zoom on the central part. Right: corresponding dispersion relation (blue crosses: experimental data, orange continuous line: parabolic fit.

By fitting the energy-momentum relation $E(p_\perp) = m_{ph}c^2 + p_\perp^2/2m_{ph}$, an effective mass m_{ph} for the photon can be estimated from the curvature term. Here, c is the speed of light in the medium and $p_\perp$ the in-plane momentum of the light. We find a photon mass $m_{ph} = (2.2881 \pm 0.0008) \times 10^{-35}$ kg. This measurement has been repeated over 43 values of pumping current between 20 and 200 mA and the mass was found to be remarkably constant $(2.28 \leq m_{ph} \leq 2.31) \times 10^{-35}$ kg. The cut-off energy of the cavity (offset term) yields an alternative method to extract the effective photon mass. Using the index of refraction as a free parameter, we obtain the same effective photon mass for a index of refraction of 3.2, consistent with the material properties of our device [32]. If strong coherent exciton-photon interactions were present the effective masses from the two methods would differ. Here they are identical, which confirms that (as expected at room temperature and for this construction) our device works with photons and not polaritons [9,33].

This dispersion relation allows us to observe the distribution of light over all the available energy band. Although this is in principle a purely spectral measurement it cannot be realized simply with an optical spectrum analyser due to the extremely large numerical aperture which

Optics EXPRESS

is required. Instead we rely on the previously determined dispersion relation and perform the measurements in the angular domain. The emitted power was measured over an approximately symmetric range of 107.8 ° by steps of 0.2 ° for 62 different pumping current values and a sample of the results is shown on Fig. 3. The data, acquired at constant solid angle of collection, has been scaled to correspond to a constant range in transverse momentum $k_\perp$. Then, one uses the dispersion relation shown on Fig. 2 to recover an energy from this value of $k_\perp$. By construction, no data is therefore available at energies below the cut-off of the dispersion relation. However, it is easily observed in Fig. 2 that the emission goes to 0 below that cutoff. At low pump (bottom three traces), the distributions fit very well a Boltzmann distribution with a constant density of states, as expected in a homogeneous two-dimensional microresonator. In Fig. 3, the continuous line is the Boltzmann law fit of the distribution observed at pumping current of 24.3 mA and it leads to a temperature of 256 K. Similar values are found for different pumping levels. This observation is crucial since the radiation temperature defined in [1] is expected to be identical to that of the medium. A slight underestimation of the actual temperature is common when inferred from light emission spectra [9,34]. Here we did not consider (for lack of detailed knowledge on the device) the lower reflectivity of the Bragg mirrors at higher k_{perp}, which may explain the underestimation. Unlike atomic systems, semiconductor media have a transparency current density below which absorption dominates over amplification. We did not observe critically different curves in our data, which may in fact all be taken above this value, only roughly estimated from material tables and geometry [35] to be about 8 mA.

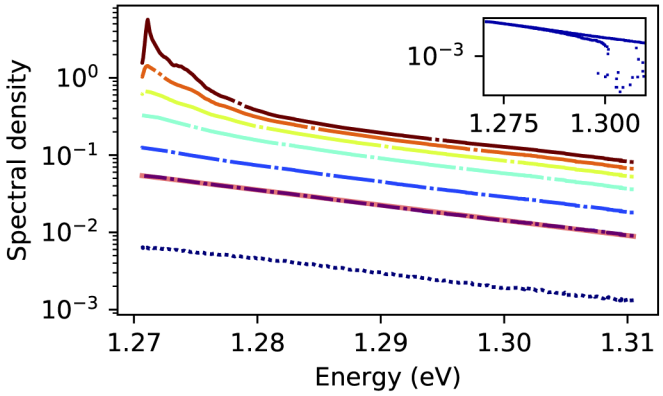

Fig. 3. Spectral density for different intracavity photon numbers. The data were acquired, from dotted dark blue (bottom) to dot- long-dashed brown (top), with pumping current values of: 4.05, 24.33, 44.60, 85.15, 125.70, 166.25, 206.79 mA respectively. Pink continuous line: exponential fit giving a temperature of 256 K. Inset: the asymmetry visible in Fig. 2 is also visible on the spectral density, which shows a cut-off on one side.

Assuming equal probability of absorption and stimulated emission, tabulated values [35] for the active region and the geometrical parameters of our device give an estimated intraband thermalization time of the order of few tens of femtoseconds. This time is extremely short compared to the photon lifetime in the resonator τ, which can be estimated from the resonator length and mirror reflectivities to be between $2.5 \leq \tau \leq 10$ ps depending on the absorption in the spacing layers and mirrors [36]. Thus, equilibrium thermalization of radiation can explain the observed spectral distribution including a radiation temperature close to that of the medium without any free parameter. In all measurements, the device's substrate is kept at constant room temperature. Although temperature is a potentially interesting control parameter, in our experiment it can be tuned only over a very small range; hence, we prefer characterizing the observations as a function of the number of photons in the resonator.

Optics EXPRESS

At higher photon density a deviation from the exponential distribution emerges close to the low-energy cut-off, while the distribution in the high-energy region remains exponential. For the two largest pumping currents (top two curves) the maximal density is not strictly in the lowest energy mode but at 1.2711 eV instead of 1.2707 eV. This observation is enabled by sub-Ångstrom resolution measurement together with extremely large numerical aperture. We attribute this tiny deviation from the exact $k_\perp = 0$ mode to spatial phenomena caused by inhomogeneities of the device. Indeed there is a region of higher photon density close to the boundaries of the active layer due to current spread and insulating boundaries (Fig. 1 left and [22]) and furthermore, the temperature profile of the device may not be constant along the radial direction due to Joule heating.

Despite a small asymmetry at high energy (Fig. 3 inset and Fig. 2), the deviation from the Boltzmann distribution at low energy is clear for both signs of $k_\perp$ and indicates the existence of a phase transition at higher values of the pumping parameter.

To characterise this phase transition we plot the spectrally resolved light intensity as a function of the total emitted light power, proportional to the intracavity photon number (Fig. 4, left). We show data for eight values of ω which correspond to emission angles of 53.2, 41.2, 29.2, 23.2, 17.2, 11.2, 5.2 and 0.2 ° from the bottom to top curves. At low total light power, the emitted light power per unit $k_\perp$ scales linearly with the total emitted power. Beyond 3mW deviations appear. The bottom three curves (highest energy) display a clear saturation while the top curves demonstrate excess population (superlinear) in the lower-energy states. Both the superlinear and the saturation are also visible when the injection current is used as horizontal axis. In this case, the total emitted power also shows the typical laser characteristic (see supplemental information). The saturation indicates that the gain clamping due to stimulated emission into the ground state causes a clamping of gain for all modes.

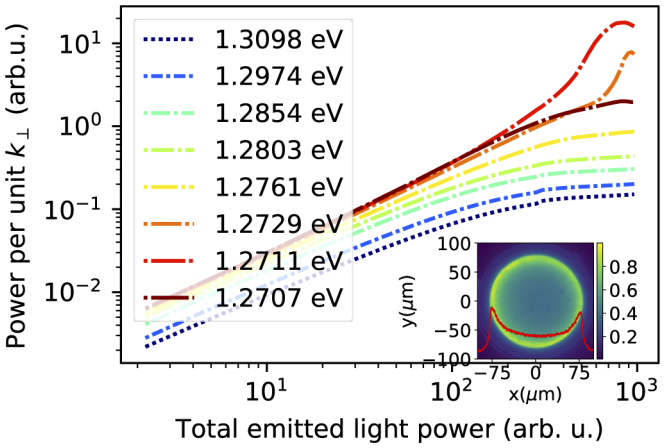

Fig. 4. Spectrally resolved light intensity as a function of the total photon number. The population excess at low energies is accompanied by a saturation in the population of the high-energy states. Inset: the image of the quantum-well region shows a much higher photon density close to the edges, very visible along the horizontal cut (continuous line).

Both the population excess at low energy and the saturation at high energy are consistent with a second-order phase transition in a finite-size system in which the whole spectrum of radiation shares the same reservoir. The most populated mode is essentially a ring close to the edge (Fig. 4, inset) most probably due to a higher current density in this region [22]. Strikingly, intraband carrier thermalization is still an effective coupling mechanism even in presence of spatial inhomogeneity.

Optics EXPRESS

To compare our observations to previous realizations of photon BEC in 2D systems [37], we first compute the thermal de Broglie wavelength $\Lambda_{th} = h/\sqrt{2\pi m k_B T}$, which for our parameters ($m = 2.28 \times 10^{-35} kg$, $T \approx 256K$) yields $\Lambda_{th} \approx 0.9\mu m$. The areal photon density ρ_{2D} at the transition can be computed from the emitted power at threshold ($P_0 = 3\,mW$), the device diameter ($\Phi = 150\ \mu$m) and the resonator lifetime τ, estimated to be between 2.5 and 10 ps, $\rho_{2D} = \frac{4P_0\tau}{\hbar\omega\pi\Phi^2}$. With these numbers, we find that the photon phase space density at threshold is of order unity with $1.7 \leq \rho_{2D}\Lambda_{th}^2 \leq 7.1$. Given the uncertainties of the parameters of the resonator, the threshold behaviour observed in Fig. 4 is thus consistent with a Bose-Einstein type transition.

The above observations are compatible with a second-order phase transition leading to a macroscopic occupation of the lowest energy band. Many open systems can exhibit a similar macroscopic occupation of a single 'quantum' state, without relying on a thermalization process. This is for instance the case for most lasers. In the present case there is no doubt that the observed equilibrium distribution is not mediated by conservative interparticle collisions, which would preserve at any time the total number of particles and would be a pure Kerr nonlinearity. Instead, we attribute thermalization, and subsequent macroscopic occupation of a single state, to particle exchange with a thermal reservoir, a process which involves all possible interactions between light and matter, including absorption and spontaneous or stimulated emission. Importantly, the latter process preserves light coherence. We also note that in our device, no parabolic confinment potential has been engineered. In an extremely large and perfectly homogeneous device, one would thus not expect BEC, but rather the appearance of a state showing either Berezinskii-Kosterlitz-Thouless (BKT) or Kardar-Parisi-Zhang (KPZ) correlations, depending on the strength of the drive and dissipation [38]. In our device, finite-size effects are known to be negligible in a strongly nonlinear regime [27,28] but residual deviations from perfect homogeneity clearly remain relevant. Further insights could be obtained via amplitude and intensity correlation measurements [39].

We have analyzed the spectral properties of an electrically pumped broad-area VCSEL and found that a Boltzmann law adequately fits spectral density over a broad range of parameters, leading to a reasonable temperature estimation. The accumulation of light in the lower-energy states when a critical intracavity photon number is reached is accompanied by saturation in the populations of high-energy states. This confirms that light thermalization through interaction with the semiconductor medium occurs throughout this phase transition which is well described by Bose-Einstein statistics. At the transition the phase-space density is of order unity, compatible with an interpretation in terms of photon BEC. These observations have been realized in a semiconductor whose only particularities are a large aspect ratio and a specific sign of detuning between resonator and luminescence maximum. This suggests that photon BEC could in fact be commonplace and that semiconductor microresonators in the weak-coupling regime are easily manufacturable sources of thermalized light, where spectral properties and phase space density can be further engineered. On a fundamental level, these devices emerge as a versatile and convenient platform for the exploration of photonic phase transitions: spatially resolved amplitude, phase and intensity correlation measurements could confirm the grand canonical conditions of the experiment and explore the possibilities of BKT or KPZ transitions. This experiment should also inspire further theoretical investigation. First the role of finite boundary conditions in a planar geometry must be carefully addressed. Second, unlike dye systems achieving light thermalization, here the medium is not made of a finite number of discrete colour centres, but, rather, of electron and hole excitations in variable numbers, thus questioning the direct applicability of existing photon thermalization theories. Recent work focussed on light emission by local equilibrium bodies [40,41] could prove particularly useful towards an adequate theoretical description of the observations reported above.

Funding. Horizon 2020 Framework Programme (820392 PhoQuS project); Engineering and Physical Sciences Research Council (EP/S000755/1).

Optics EXPRESS

Disclosures. The authors declare no conflicts of interest.

References

1. P. Würfel, "The chemical potential of radiation," J. Phys. C: Solid State Phys. **15**(18), 3967–3985 (1982).
2. L. A. Lugiato and R. Lefever, "Spatial dissipative structures in passive optical systems," Phys. Rev. Lett. **58**(21), 2209–2211 (1987).
3. R. Y. Chiao and J. Boyce, "Bogoliubov dispersion relation and the possibility of superfluidity for weakly interacting photons in a two-dimensional photon fluid," Phys. Rev. A **60**(5), 4114–4121 (1999).
4. J. Klaers, F. Vewinger, and M. Weitz, "Thermalization of a two-dimensional photonic gas in a 'white wall' photon box," Nat. Phys. **6**(7), 512–515 (2010).
5. J. Kasprzak, M. Richard, S. Kundermann, A. Baas, P. Jeambrun, J. Keeling, F. Marchetti, M. Szymańska, R. Andre, J. Staehli, V. Savona, P. B. Littlewood, B. Deveaud, and L. S. Dang, "Bose–Einstein condensation of exciton polaritons," Nature **443**(7110), 409–414 (2006).
6. K. Daskalakis, S. Maier, R. Murray, and S. Kéna-Cohen, "Nonlinear interactions in an organic polariton condensate," Nat. Mater. **13**(3), 271–278 (2014).
7. J. D. Plumhof, T. Stöferle, L. Mai, U. Scherf, and R. F. Mahrt, "Room-temperature Bose–Einstein condensation of cavity exciton–polaritons in a polymer," Nat. Mater. **13**(3), 247–252 (2014).
8. Y. Sun, P. Wen, Y. Yoon, G. Liu, M. Steger, L. N. Pfeiffer, K. West, D. W. Snoke, and K. A. Nelson, "Bose-einstein condensation of long-lifetime polaritons in thermal equilibrium," Phys. Rev. Lett. **118**(1), 016602 (2017).
9. J. Klaers, J. Schmitt, F. Vewinger, and M. Weitz, "Bose-einstein condensation of photons in an optical microcavity," Nature **468**(7323), 545–548 (2010).
10. J. Marelic and R. A. Nyman, "Experimental evidence for inhomogeneous pumping and energy-dependent effects in photon Bose-Einstein condensation," Phys. Rev. A **91**(3), 033813 (2015).
11. S. Greveling, K. L. Perrier, and D. van Oosten, "Density distribution of a bose-einstein condensate of photons in a dye-filled microcavity," Phys. Rev. A **98**(1), 013810 (2018).
12. T. K. Hakala, A. J. Moilanen, A. I. Väkeväinen, R. Guo, J.-P. Martikainen, K. S. Daskalakis, H. T. Rekola, A. Julku, and P. Törmä, "Bose–einstein condensation in a plasmonic lattice," Nat. Phys. **14**(7), 739–744 (2018).
13. P. Kirton and J. Keeling, "Nonequilibrium model of photon condensation," Phys. Rev. Lett. **111**(10), 100404 (2013).
14. R. Weill, A. Bekker, B. Levit, M. Zhurahov, and B. Fischer, "Thermalization of one-dimensional photon gas and thermal lasers in erbium-doped fibers," Opt. Express **25**(16), 18963–18973 (2017).
15. R. Weill, A. Bekker, B. Levit, and B. Fischer, "Bose–einstein condensation of photons in an erbium–ytterbium co-doped fiber cavity," Nat. Commun. **10**(1), 747 (2019).
16. C. Conti, M. Leonetti, A. Fratalocchi, L. Angelani, and G. Ruocco, "Condensation in disordered lasers: theory, 3 d+ 1 simulations, and experiments," Phys. Rev. Lett. **101**(14), 143901 (2008).
17. J. Huang, C. Liu, Y. Zhu, S. Masala, E. Alarousu, Y. Han, and A. Fratalocchi, "Harnessing structural darkness in the visible and infrared wavelengths for a new source of light," Nat. Nanotechnol. **11**(1), 60–66 (2016).
18. R. Michalzik, *VCSELs: fundamentals, technology and applications of vertical-cavity surface-emitting lasers*, vol. 166 (Springer, 2012).
19. H. Moench, R. Conrads, C. Deppe, G. Derra, S. Gronenborn, X. Gu, G. Heusler, J. Kolb, M. Miller, P. Pekarski, J. Pollmann-Retsch, A. Pruijmboom, and U. Weichmann, "High-power VCSEL systems and applications," Proc. SPIE **9348**, 93480W (2015).
20. L. Spinelli, G. Tissoni, M. Brambilla, F. Prati, and L. Lugiato, "Spatial solitons in semiconductor microcavities," Phys. Rev. A **58**(3), 2542–2559 (1998).
21. S. P. Hegarty, G. Huyet, J. G. McInerney, and K. D. Choquette, "Pattern formation in the transverse section of a laser with a large fresnel number," Phys. Rev. Lett. **82**(7), 1434–1437 (1999).
22. T. Ackemann, S. Barland, M. Cara, S. Balle, J. Tredicce, R. Jäger, M. Grabherr, M. Miller, and K. J. Ebeling, "Spatial mode structure of bottom-emitting broad-area vertical-cavity surface-emitting lasers," J. Opt. B: Quantum Semiclassical Opt. **2**(3), 406–412 (2000).
23. S. Barland, J. R. Tredicce, M. Brambilla, L. A. Lugiato, S. Balle, M. Giudici, T. Maggipinto, L. Spinelli, G. Tissoni, T. Knödl, M. Miller, and R. Jäger, "Cavity solitons as pixels in semiconductor microcavities," Nature **419**(6908), 699–702 (2002).
24. Y. Tanguy, T. Ackemann, W. Firth, and R. Jäger, "Realization of a semiconductor-based cavity soliton laser," Phys. Rev. Lett. **100**(1), 013907 (2008).
25. S. Barbay, X. Hachair, T. Elsass, I. Sagnes, and R. Kuszelewicz, "Homoclinic snaking in a semiconductor-based optical system," Phys. Rev. Lett. **101**(25), 253902 (2008).
26. P. Genevet, S. Barland, M. Giudici, and J. R. Tredicce, "Bistable and addressable localized vortices in semiconductor lasers," Phys. Rev. Lett. **104**(22), 223902 (2010).
27. T. Ackemann, W. Firth, and G.-L. Oppo, "Fundamentals and applications of spatial dissipative solitons in photonic devices," Adv. At., Mol., Opt. Phys. **57**, 323–421 (2009).
28. S. Barbay, R. Kuszelewicz, and J. Tredicce, "Cavity solitons in vcsel devices," Adv. Opt. Technol. **2011**, 1–23 (2011).
29. R. Bhattacharya, B. Pal, and B. Bansal, "On conversion of luminescence into absorption and the van roosbroeck-shockley relation," Appl. Phys. Lett. **100**(22), 222103 (2012).

Optics EXPRESS

30. M. Grabherr, R. Jager, M. Miller, C. Thalmaier, J. Herlein, R. Michalzik, and K. J. Ebeling, "Bottom-emitting VCSEL's for high-cw optical output power," IEEE Photonics Technol. Lett. **10**(8), 1061–1063 (1998).
31. R. Michalzik, M. Grabherr, and K. J. Ebeling, "High-power vcsels: modeling and experimental characterization," in *Vertical-cavity surface-emitting lasers II*, vol. 3286 (1998), pp. 206–219.
32. At $\lambda = 1\ \mu m$, $n = 3.5;3.0;3.0$ for GaAs, $Al_{0.9}Ga_{0.1}As$ and AlGaAs, respectively.
33. J. Marelic, B. T. Walker, and R. A. Nyman, "Phase-space views into dye-microcavity thermalized and condensed photons," Phys. Rev. A **94**(6), 063812 (2016).
34. B. T. Walker, L. C. Flatten, H. J. Hesten, F. Mintert, D. Hunger, A. A. Trichet, J. M. Smith, and R. A. Nyman, "Driven-dissipative non-equilibrium bose–einstein condensation of less than ten photons," Nat. Phys. **14**(12), 1173–1177 (2018).
35. L. A. Coldren and S. W. Corzine, *Diode Lasers and Photonic Integrated Circuits* (Wiley, New York, 1995).
36. R. Michalzik and K. J. Ebeling, "Operating principles of vcsels," in *Vertical-Cavity Surface-Emitting Laser Devices*, (Springer, 2003), pp. 53–98.
37. T. Damm, D. Dung, F. Vewinger, M. Weitz, and J. Schmitt, "First-order spatial coherence measurements in a thermalized two-dimensional photonic quantum gas," Nat. Commun. **8**(1), 158 (2017).
38. E. Altman, L. M. Sieberer, L. Chen, S. Diehl, and J. Toner, "Two-dimensional superfluidity of exciton polaritons requires strong anisotropy," Phys. Rev. X **5**(1), 011017 (2015).
39. J. Schmitt, T. Damm, D. Dung, F. Vewinger, J. Klaers, and M. Weitz, "Observation of grand-canonical number statistics in a photon bose-einstein condensate," Phys. Rev. Lett. **112**(3), 030401 (2014).
40. J.-J. Greffet, P. Bouchon, G. Brucoli, and F. Marquier, "Light emission by nonequilibrium bodies: local kirchhoff law," Phys. Rev. X **8**(2), 021008 (2018).
41. L. Wojszvzyk, H. Monin, and J.-J. Greffet, "Light emission by a thermalized ensemble of emitters coupled to a resonant structure," Adv. Opt. Mater. **7**(14), 1801697 (2019).